VOL. 22, NO. 2, 2023, 22-29
elektrika.utm.my
ISSN 0128-4428

ELEKTRIKA
Journal of Electrical Engineering

Supervisory Control of Solar-Wind-Biomass-Fuel Cell Energy System for Optimal Performance

Babangida Modu[1,3], **Md Pauzi Abdullah**[1,2*], **Abba Lawan Bukar**[3], **Musa Mustapha**[3]

[1]Centre of Electrical Energy Systems, Faculty of Electrical Engineering, Universiti Teknologi Malaysia, UTM, 81310 Skudai, Johor, Malaysia.
[2]Institute of Future Energy, Universiti Teknologi Malaysia, UTM, 81310 Skudai, Johor, Malaysia.
[3]Department of Electrical and Electronic Engineering, University of Maiduguri, 1069 Maiduguri, Borno, Nigeria.

[*]Corresponding author: mpauzi@utm.my

Abstract: Generating electricity through a hybrid renewable energy system (HRES) plays a crucial role in achieving the sustainable development goal of affordable and clean energy (SDG 7). However, designing an optimal HRES is challenging due to the fluctuating demand and intermittent nature of renewable energy sources (RES). In recent times, hybrid hydrogen-battery energy storage technologies have garnered significant attention as they offer a pathway to a sustainable HRES with zero net emissions. This research paper introduces a rule-based algorithm and a metaheuristic optimization technique called Levy Flight Algorithm (LFA) for the energy management strategy (EMS) of an independent HRES. The EMS aims to establish a sequence for power delivery among the different components within the microgrid. The LFA is employed to optimize this EMS. To account for the variability and unpredictability of renewable energy sources, the proposed EMS is evaluated across four scenarios: winter, spring, summer, and autumn. These scenarios are derived from a stochastic model of RES. The results of the evaluation demonstrate that the energy management strategy implemented to control the HRES has successfully established an environmentally friendly energy system.

Keywords: Hydrogen fuel cell, Renewable energy sources, Supervisory control, Levy flight algorithm

Article History: received 3 July 2023; accepted 3 August 2023; published 28 August 2023.

1. INTRODUCTION

The depletion of fossil fuel reserves, coupled with increasing concerns about climate change and global warming, has prompted serious concerns about conventional energy systems. In response to these challenges, renewable energy sources (RESs) have emerged as promising alternatives to replace inefficient fossil fuel-based systems. These RESs offer enhanced viability and environmental friendliness, providing a sustainable and innovative solution to conventional energy systems[1-3]. Renewable energy sources (RESs) provide multiple advantages, including improved energy supply security, reduced greenhouse gas emissions, expanded energy markets, and decreased reliance on imported energy in remote areas. Moreover, the adoption of renewable energy (RE) systems has the potential to stimulate economic growth, create employment opportunities, and enhance overall human well-being. However, the intermittent nature of RE sources like solar and wind energy, which rely on climatic conditions, presents a significant challenge to their widespread implementation[4, 5]. For the seamless integration of renewable energy sources (RES) and energy storage systems (ESS) in microgrids, a carefully designed and coordinated energy management scheme (EMS) is essential to avoid unnecessary costs. Numerous studies have explored the effective management and capacity of hybrid renewable energy systems, which integrate hydrogen fuel cells and battery storage[6]. These studies have employed different approaches and viewpoints to determine the best strategies.

The researchers in reference [7] utilized ant colony optimization to address the challenge of optimizing the size of a standalone microgrid that combines photovoltaic (PV) and wind energy sources. The article referenced as [8] describes the utilization of a genetic algorithm (GA) to determine the optimal location and size for a compact microgrid setup. This microgrid configuration incorporates various components such as wind turbines, photovoltaic panels, a biodiesel generator, an energy storage system electrolyzer, a fuel cell, a hydrogen storage tank, and a lead-acid battery. The authors of [9] suggest using the LCOE as the main criterion for determining the size of an off-grid system. This system consists of a PV unit, a wind turbine (WT), a battery storage system, and an electrolyzer. Additionally, the authors created an EMS to regulate the power usage of these different distributed energy components. In the study cited as [10], the researchers devised different operational approaches and discovered that the hydrogen based storage system demonstrated superior performance compared to battery storage system. The study cited as [11] examined the benefits of utilizing a hybrid energy storage system that

combines both hydrogen and battery energy storage. The authors acknowledged that battery storage is more cost-effective and, when combined with hydrogen storage, can effectively handle the uncertainties associated with renewable energy and loads. The authors emphasized that hydrogen, being a reliable and environmentally friendly energy storage solution, is highly compatible with battery storage for energy dispatch purposes. The study referenced as [12] examined the cost of hydrogen produced through electrolysis and aimed to minimize the price of hydrogen supply. The study's model successfully determined the optimal configuration of a hybrid system by effectively utilizing wind, solar, and geothermal energy resources. In the study referred to as[13] the authors investigated the influence of the wind capacity factor and electricity cost, specifically focusing on evaluating the production cost of hydrogen. However, the study solely examined the cost of hydrogen production and did not evaluate the overall economic feasibility of hydrogen energy storage systems (HESS). The study cited as [12] analysed the levelized cost of hydrogen from electrolysis and minimised the hydrogen supply price. The authors of the study cited as [13] examined the impact of the wind capacity factor and cost of electricity, but they only focused on analysing the cost of hydrogen production without evaluating the overall economic feasibility of hydrogen energy storage systems (HESS). Fuel cells generate electricity by utilizing the electrochemical reaction of hydrogen and oxygen, with the hydrogen produced or consumed stored in the hydrogen storage tank (HST). As a result, both the costs of hydrogen production and fuel cell operation when assessing the economic viability of HESS. In [14], the authors conducted a technical and economic evaluation to explore the generation of power and hydrogen through a hybrid system utilizing solar and wind energy. Their study demonstrated that to get a very reliable system, the optimal LCOE was found to be 0.50 $/kWh. In reference [15], the authors conducted a comparison between two systems: an off-grid system using PV/WT/battery and another system using PV/WT/hydrogen storage.

It is clear from the literature mentioned above that several renewable energy sources were used for the hybrid renewable energy system optimisation. The main contributions of the paper are summarized as follows:

- Development of a mathematical model to optimize the capacity of a hybrid renewable energy system, including solar, wind, biomass, hydrogen fuel cell, and battery storage with a view to reduce costs while evaluating the effectiveness of the HRES based on the annualized system cost and the probability of power supply loss.
- The use of meta heuristic Levy Flight Algorithm (LFA) to configure a standalone hybrid renewable energy system. This algorithm is utilized to optimize the distribution of power among the different components.
- Application of the proposed method to address the optimal configuration of a standalone HRES in an isolated community. The study incorporates real resources and load data obtained from a meteorological agency and an electricity regulatory commission.

2. DESCRIPTION OF THE PROPOSED HRES

A schematic diagram of the hybrid system is presented in Figure 1. To address the intermittent nature of power generation from REs, the microgrid incorporates two energy storage systems: hydrogen storage and battery storage. The DC power obtained from the DC bus can be converted into AC power using an inverter to fulfil the electrical load requirements. Excess DC power can be either stored in a battery or transformed into hydrogen using an electrolyzer. The produced hydrogen can be compressed and stored for future use when the energy supply is inadequate. The fuel cell can generate DC power by combining hydrogen with oxygen.

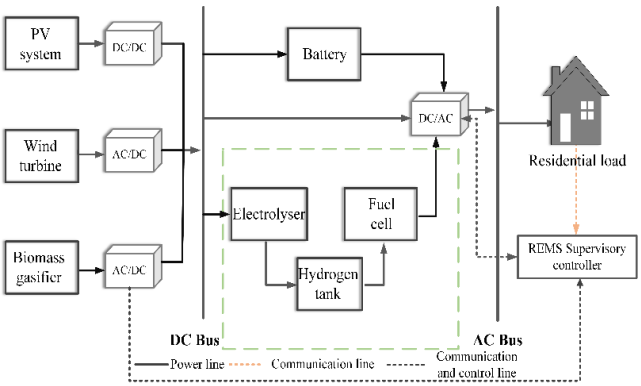

Figure 1 The studied stand-alone HRES configuration

2.1 Solar photovoltaic model

The energy output per unit of PV panel can be calculated using the following equations[4, 16]:

$$P_{pv\_out} = P_{N\_PV} \times \frac{G}{G_{ref}}\left[1 + K_t\left((T_{amb} + (0.0256 \times G)) - T_{ref}\right)\right] \quad (1)$$

where, P_{pv_out} is the output power of the photovoltaic panel, P_{N_PV} references power under reference condition, G_{ref} is 1000 W/m^2, G is the solar insolation (W/m^2), K_t is $-3.7 * 10^{-3}(1/oC)$, T_{ref} is 25°C and T_{amb} is the ambient temperature.

2.2 Wind turbine model

The power produced by a wind turbine is influenced by several factors such as the rated power of the turbine, the cut-in wind speed, the cut-out wind speed, and the rated wind speed. A mathematical model can be used to define the power output of the individual turbine based on these factors as:

$$P_{WT-out}(t) = \begin{cases} 0 & V<V_{cut-in} \text{ and } V>V_{cut-out} \\ aV^3 - bP_r & V_{cut-in}<V>V_{Rated} \\ P_r & V_{rated}<V<V_{cut-out} \end{cases} \quad (2)$$

where P_r is the rated power, a and b are constants and can be expressed as:

$$a = \frac{P_r}{(V_{Rated}^3 - V_{cut-in})} \quad (3)$$

$$b = \frac{V_{cut-in}^3}{(V_{Rated}^3 - V_{cut-in}^3)} \quad (4)$$

2.3 Biomass model

The equation below can be used to calculate the annual electricity output (E_{bmg}) of the biomass gasifier:

$$E_{bmg} = P_{bmg} \times (8760 - CUF) \quad (5)$$

where P_{bmg} stand for rating of the biomass gasifier and CUF is the capacity utilization factor.

The maximum rating of a biomass installed in a given area can be obtain using Equation (6) as:

$$P_{bmg}^m = \frac{Totol\ biomass\ available(Ton/yr) \times 1000 \times CV_{bm} \times \eta_{bmg}}{365 \times 860 \times Operating\ hours/day} \quad (6)$$

The general efficiency of converting biomass into electricity is represented by η_{bmg}, and CV_{bm} stands for the calorific value of the specific biomass being used[17].

2.4 Hydrogen storage model

The energy supply from electrolyzer to H_2 tanks is expressed as in Equation (7):

$$P_{el-ht} = P_{ren-el} \times \eta_{el} \quad (7)$$

where P_{el-ht} stands for power output of the electrolyser, P_{ren-el} is renewable energy supplied to the electrolyser, and η_{el} is the of the efficiency electrolyser.

The subsequent equations represent the state of the hydrogen storage tank at each time t [18].

$$E_{ht}(t) = E_{ht}(t-1) + P_{ren-el}(t) \times \Delta t - P_{ht-fc}(t) \times \Delta t \times \eta_{ht} \quad (8)$$

$$M_{ht}(t) = \frac{E_{ht}(t)}{HHV_{H_2}} \quad (9)$$

$E_{ht}(t)$ and $E_{ht}(t-1)$ refer to the stored energy in the tank at time t and $t-1$, in that order, P_{ht-fc} stand for the amount of energy supplied to the fuel cell from the hydrogen tank at the time t, η_{ht} is the efficiency of hydrogen tank, and Δt refers to time interval, which is 1 hour in this case. In addition, $M_{ht}(t)$ represents the mass of hydrogen supplied to hydrogen tank, and HHV_{H_2} is a designate utilized to indicate the calorific value of hydrogen, which is 39.72 kWh/Kg.umber citations consecutively in square brackets. Please note that the references at the end of this document are in the preferred reference style. Give all authors' names; Use a space after authors' initials. Capitalize only the first word in a paper title, except for proper nouns and element symbols.

2.5 Battery model

The energy from the renewable systems is unpredictable and may generate in excess or less than required. This excess or deficit in energy generation shows if the battery is receiving or releasing power, which is represented by Equation (10) as:

$$P_B(t) = (P_{PV}(t) + P_{WT}(t)) - \frac{P_L(t)}{n_{inv}} \quad (10)$$

n_{inv} refer to the inverter's efficiency. If $P_B(t) > 0$, it means that the renewable energy systems generate more than required, while $P_B(t) < 0$ indicates a shortage of power generation. The battery only charges when there is surplus generation or when the state of charge (SoC) is below maximum SoC (SoC_{max}). Likewise, Equation (11) represents the SoC of the battery in charging at time t[19].

$$SoC(t) = SoC(t-1)(1-\sigma) + ((P_{PV}(t) + P_{WT}(t)) - \frac{P_L(t)}{n_{inv}}) \times n_B \quad (11)$$

Here σ is the battery's hourly self-discharge rate and n_B symbolizes the battery's efficiency[20, 21].

When renewable generation is not enough and the battery is above its maximum permissible SoC (i.e.,$SoC(t) < SoC_{min}$), the battery storage is discharged to meet demand in accordance with Equation (12).

$$SoC(t) = SoC(t-1)(1-\sigma) - (\frac{P_L(t)}{n_{inv}} - (P_{PV}(t) + P_{WT}(t))) \times n_B \quad (12)$$

2.6 Supervisory control

Supervisory control algorithm is used to achieve power flow management in this study. There are three main types of these algorithms: Optimization-Based, Learning-Based, and Rule-Based. Each algorithm operates differently and yields varying degrees of accuracy in its results. In the context of the study being discussed, the rule-based EMS algorithm has been specifically chosen. Figure (2a) and (2b) depict a simplified flow chart that illustrates the operational strategy of the proposed hybrid energy system.

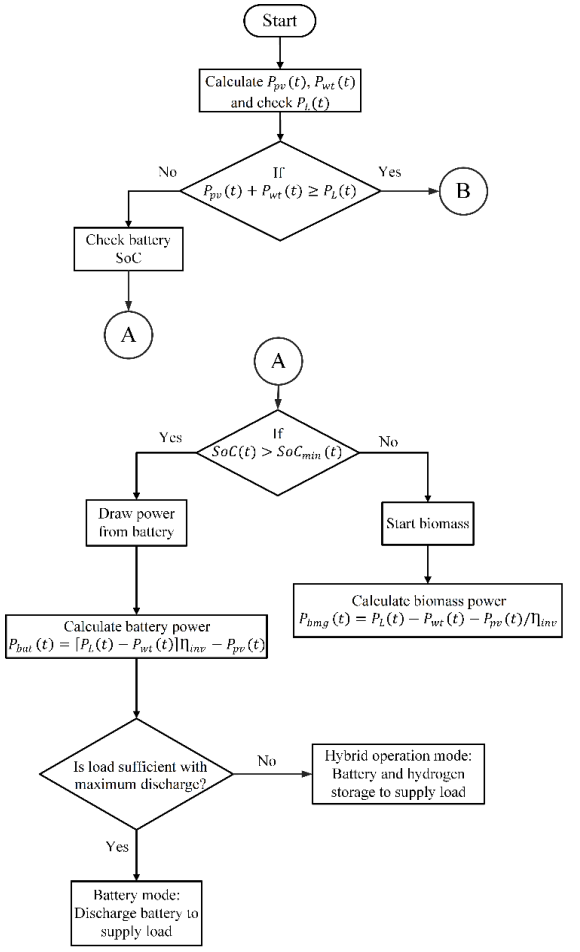

Figure 2a Energy management Strategy

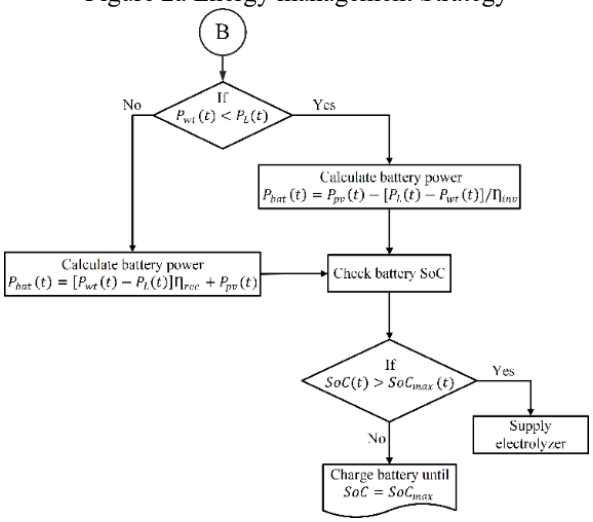

Figure 2b Energy management strategy

3. OBJECTIVE FUNCTION

The primary goal of this study is to reduce the overall ASC of the suggested hybrid system while ensuring an optimal energy transfer.

The function represented by Equation 13 is regarded as the primary objective function that must be minimised while keeping constraints in mind.

$$ASC(\$/kWh) = F(N_{pv}C_{pv} + N_{wt}C_{wt} + N_{bat}C_{bat} + N_{ele}C_{ele} + N_{ht}C_{ht} + P_{fc}C_{fc} + P_{bmg}C_{bmg} + P_{inv}C_{inv}) \quad (13)$$

where the costs for photovoltaic panel, wind turbines, biomass, electrolyser, hydrogen tank, fuel cell stack, batteries, and inverters are given as C_{pv}, C_{wt}, C_{bmg}, C_{ele}, C_{ht}, C_{fc}, C_{bat}, and C_{inv} respectively. N_{pv}, N_{wt}, N_{bat}, N_{ele}, and N_{ht} represent the number of photovoltaic, wind turbine, battery, electrolyser, and hydrogen tanks. The ratings of the biomass gasifier, fuel cell stack and inverter are represented by P_{bmg}, P_{fc}, and P_{inv} respectively.

LCOE and reliability are used to determine which configuration is best. The LCOE of system which is defined as the average cost per kWh of the energy it produces, can be expressed as in Equation (14),

$$LCOE = \frac{ASC(\$/year)}{Total\ useful\ energy\ served(kWh/year)} \quad (14)$$

The LPSP is used in this research to evaluate the reliability of the standalone HRES. It is given by Equation (15):

$$LPSP = \frac{\sum LPS}{\sum P_{Load}} \quad (15)$$

4. LEVY FLIGHT ALGORITHM (LFA)

The Levy flight is a probability distribution put forth by Paul Pierre Lévy, a French mathematician in the 1930s[22]. Levy flight mechanism acts as a global searching operator and employs short-distance walking in combination with long-distance jumping routes to explore the search space. An outline of the proposed LFA algorithm to solve the problem is given below:

Algorithm

Step 1: Load input data:

a) Load the meteorological database which contains information on the wind, solar irradiation, and ambient temperature.
b) The database of the load requirement.
c) Load the database of the techno-economic specifications of the microgrid elements as given in table 2.
d) Load the database of the economic indicators which include lifetime, interest rate and inflation of the project in accordance with the specification.

Step 2: Initialize algorithm parameters:

a) LFA constants:
   - Population size $n = 40$, number of iterations $T = 100$, step size control factor $a = 0.01$.
b) Set constraints:
   - LPSP according to Eq. (15)
c) Set the search space:
   - The minimum and maximum limits for the number of photovoltaic (PV) modules [0 50].
   - The minimum and maximum limits for the number of wind turbines (WT) modules [0 10].

Step 3: Calculate the fitness value of each search individual and treat the individual with the best fitness value in the current population as food.

Step 4: Update the best solution using Equation (15),

$$X_i(t+1) = X_i(t) + S\ \Phi\ X_i(t) \quad (15)$$

Step 5: Perform Levy flight steps by generating a random step length and direction based on the Levy flight distribution using Equation (16),

$$S = \frac{u}{|v|^{1/\beta}} \tag{16}$$

Step 6: Evaluate the fitness of the new candidate solutions obtained from the Levy flight steps.

Step 7: Update the population by replacing the previous solutions with new ones.

Step 8: Check if the algorithm has either reached its maximum allowed iterations or discovered the best possible solution. If the end condition of the algorithm is met, return the optimal value and exit; if not, proceed to Step 3.

5. RESULTS AND DISCUSSION

This section is designated to discuss the achieved outcome of the rule-based supervisory control of the HRES. The system incorporates two primary renewable energy sources (RESs), which are integrated with hydrogen fuel cell and battery storage. Figure (3a) and (3b) display the power output derived from the photovoltaic and wind turbine systems, as calculated using Equations (1) and (2) respectively. The output power from the photovoltaic system is determined based on the prevailing climatic conditions, primarily taking into account the ambient temperature (T_{amb}) and solar irradiance (G). The output power from the wind turbine is influenced by the cut-in speed (v_{cut-in}), cut-out speed ($v_{cut-out}$), and rated speed (v_r), which are specified by the manufacturer.

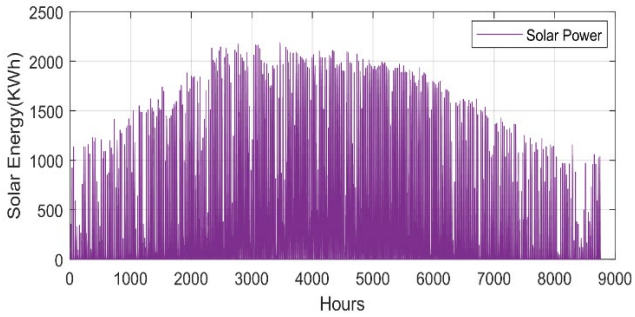

Figure 3a Generated Output Power from solar for one year.

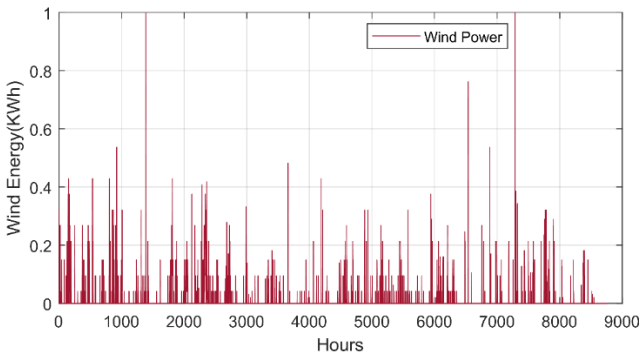

Figure 3b Output power generated from WT for one year.

Figure (4a), (4b), (4c), and (4d) present visual representations of the energy balance between energy demand and supply over different time periods, with each figure corresponding to a specific season.

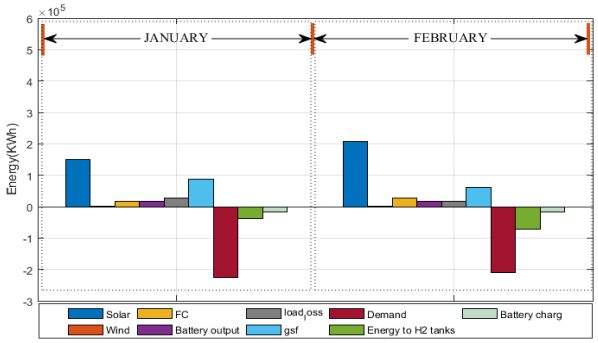

Figure 4a Energy balance between demand and supply in winter season

In spring season, Figure 4b demonstrates a notable increase in power generation from photovoltaic systems as a result of higher solar radiation during this season. This indicates normal climate conditions without sudden changes, such as large cloud coverage. However, despite this increase in solar energy output, the combined renewable energy generated is still not enough to meet the load demand. Furthermore, the energy produced by the combined storage system (hydrogen fuel cell and battery storage) cannot cover the deficit, even with the increased output from the hydrogen fuel cell. To compensate for the energy shortfall, biomass power generation is employed to bridge the gap and ensure the load requirements are met during the spring season.

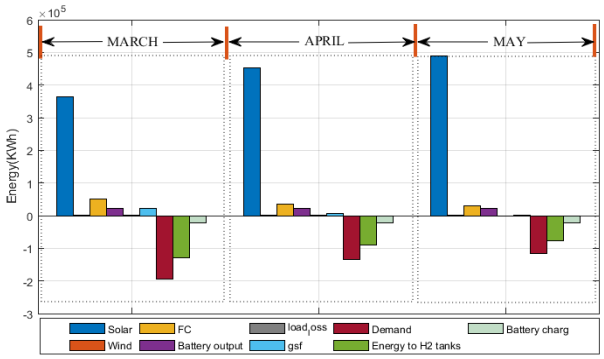

Figure 4b Energy balance between demand and supply in spring season

In the summer season, Figure 4c reveals that photovoltaic systems generate the highest amount of renewable energy due to the abundance of solar radiation. Particularly in June and August, the renewable energy generated, especially from photovoltaic sources, is sufficient to meet the load demand. The excess energy generated is utilized to charge the battery storage system and supply the electrolyzer for hydrogen production. Biomass power generation is only required for a few hours in the month of July.

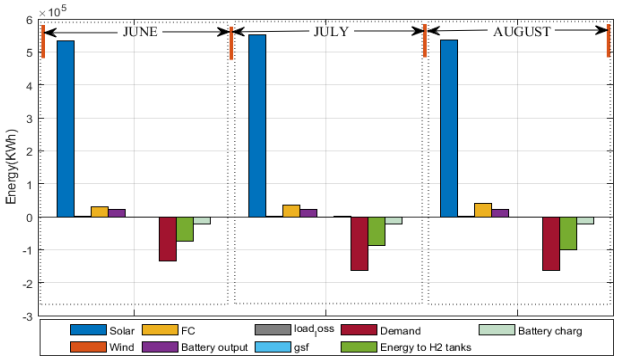

Figure 4c Energy balance between demand and supply in summer season

As for the autumn season, Figure 4d shows a decrease in power generation from renewable sources, particularly from September to November. This decrease is primarily attributed to lower solar radiation and haze during this season. Consequently, the reliance on biomass power generation to meet the load demand increases as the autumn season progresses from the beginning to the end.

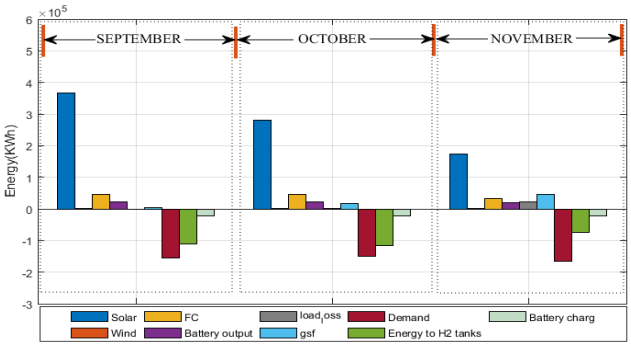

Figure 4d Energy balance between demand and supply in autumn season

To provide a more user-friendly representation of the energy flow in the optimized system, Figure 5 represents the hourly output of each technology for a typical week in the first quarter of the year. The dispatch profile during this week reveals an excess of renewable energy, particularly at noon. This surplus energy is utilized to charge the battery bank, operate the electrolyzer for hydrogen generation, and supply the fuel cell during peak hours and times of reduced renewable generation. In instances where renewable energy output falls short of meeting the load demand, the fuel cell and battery storage compensate for the unmet load. These processes alternate to achieve a dynamic energy balance within the microgrid system.

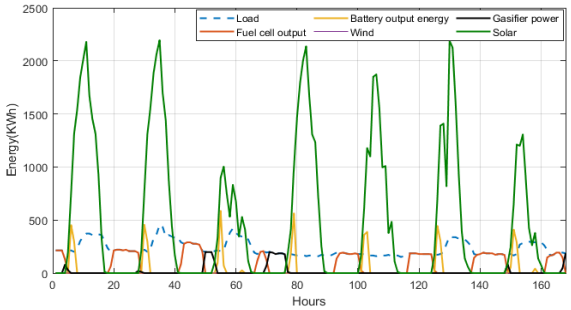

Figure 5 Hourly output of the component of the HRES in a typical week.

To verify the optimal operation of the proposed system over the course of a year, a selected period of one week is examined in detail. Additionally, 50 specific hours within this week are taken into consideration for analysis. Figure 6 illustrates the complete power exchange that occurs during this one-week period. The figure shows that during certain hours within the considered week (0049-0053, 0069-0077, and 0166-0168), solar and wind power generation is low, and the battery SoC is approaching the minimum threshold. Consequently, during these specific hours, the biomass gasifier is utilized to supply power to the system and compensate for the energy deficit.
Figure 7 presents the EMS analysis on the selected 50 hours within the week. It can be deduced that a significant amount of solar power is generated during these hours due to favourable solar resource availability. Therefore, there is no need for biomass power generation.

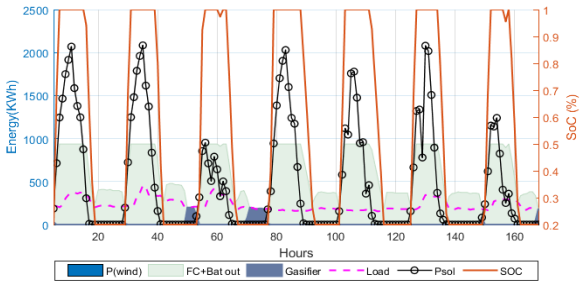

Figure 6 Energy balance and battery SoC for a week.

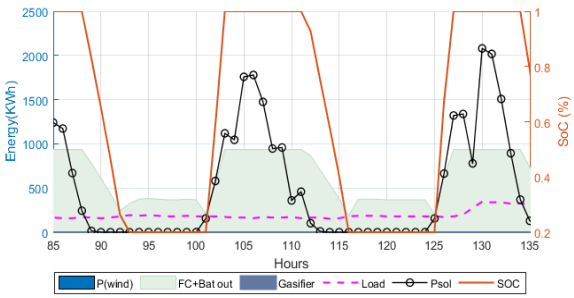

Figure 7 Daily energy balance and battery SoC

Figure 8 depicts a visual interpretation of the optimization results for the annualized system cost of the HRES components. The aim of these optimizations is to determine the optimal outcomes for ASC and LCOE of the HRES. Additionally, the reliability constraints are taken into account throughout the project's length. The optimized setup produces an ASC of 1.85996 million dollars (M$), an LCOE of 0.9342 dollars per kilowatt-hour ($/kWh) and guarantees a maximum LPSP of just 5%.

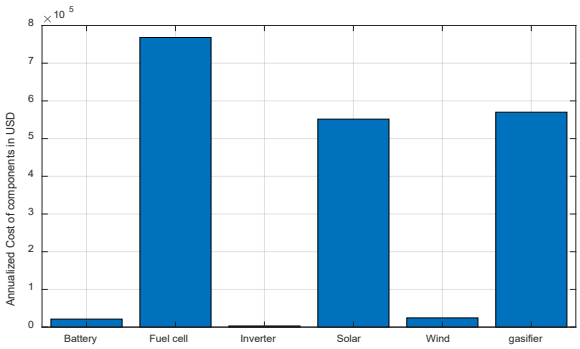

Figure 8 Annualized system cost of the HRES components

6. CONCLUSION

In this research, a theoretical HRES that operates independently of the main power grid was examined to validate the effectiveness of the proposed Energy Management Strategy (EMS). The purpose of this HRES is to fulfill the energy requirements of an off-grid community. The renewable energy sources within the HRES can be adjusted based on the renewable energy potential of different areas. Consequently, solar photovoltaic (PV) and wind turbines (WT) were prioritized as the primary sources of energy in the HRES. Subsequently, the REMS was implemented to give priority to the utilization of renewable energy sources and manage the power flow among the different components of the microgrid. This implementation aimed to emphasize the effectiveness of the Levy Flight Algorithm (LFA) in solving the specific problem being addressed. The findings of the research indicate that the proposed scheme successfully manages a seamless power flow within the HRES using the same optimal configuration. It also demonstrated that the proposed approach presents a viable and environmentally sustainable solution for electrifying off-grid communities. This suggests that the combination of the HRES, EMS, REMS, and the utilization of renewable energy sources can effectively fulfill the energy requirements of off-grid communities while being environmentally friendly.

ACKNOWLEDGMENT

The authors gratefully acknowledge Universiti Teknologi Malaysia (UTM) for providing access to library facilities. Additionally, we extend our heartfelt appreciation to all the individuals who have contributed, directly or indirectly, to the development of this article.

REFERENCES

[1] B. Modu, A. Aliyu, A. Bukar, M. Abdulkadir, Z. Gwoma, and M. Mustapha, "Techno-economic analysis of off-grid hybrid pv-diesel-battery system in Katsina State, Nigeria," *Arid Zone Journal of Engineering, Technology and Environment,* vol. 14, no. 2, p. 317, 2018.

[2] B. Modu, M. P. Abdullah, and A. L. Bukar, "Hybrid Reaching Law-Based Integral Sliding Mode Control for DC Microgrid," in *2022 IEEE 20th Student Conference on Research and Development (SCOReD)*, 2022: IEEE, pp. 92-95.

[3] N. Bashir, B. Modu, and P. Harcourt, "Techo-economic analysis of off-grid renewable energy systems for rural electrification in North-eastern Nigeria," *International Journal of Renewable Energy Research (IJRER),* vol. 8, no. 3, pp. 1217-1228, 2018.

[4] A. L. Bukar, C. W. Tan, L. K. Yiew, R. Ayop, and W.-S. Tan, "A rule-based energy management scheme for long-term optimal capacity planning of grid-independent microgrid optimized by multi-objective grasshopper optimization algorithm," *Energy conversion and management,* vol. 221, p. 113161, 2020.

[5] B. Modu, M. P. Abdullah, M. A. Sanusi, and M. F. Hamza, "DC-based microgrid: Topologies, control schemes, and implementations," *Alexandria Engineering Journal,* vol. 70, pp. 61-92, 2023.

[6] B. Modu, M. P. Abdullah, A. L. Bukar, and M. F. Hamza, "A systematic review of hybrid renewable energy systems with hydrogen storage: Sizing, optimization, and energy management strategy," *International Journal of Hydrogen Energy,* 2023/06/29/ 2023, doi:

[7] A. Fetanat and E. Khorasaninejad, "Size optimization for hybrid photovoltaic–wind energy system using ant colony optimization for continuous domains based integer programming," *Applied Soft Computing,* vol. 31, pp.

[8] P. Nagapurkar and J. D. Smith, "Techno-economic optimization and environmental Life Cycle Assessment (LCA) of microgrids located in the US using genetic algorithm," *Energy Conversion and Management,* vol. 181, pp. 272-291, 2019.

[9] D. Zhao *et al.*, "Capacity optimization and energy dispatch strategy of hybrid energy storage system based on proton exchange membrane electrolyzer cell," *Energy Conversion and Management,* vol. 272, p.

[10] Y. Zhang, P. E. Campana, A. Lundblad, and J. Yan, "Comparative study of hydrogen storage and battery storage in grid connected photovoltaic system: Storage sizing and rule-based operation," *Applied energy,* vol. 201, pp. 397-411, 2017.

[11] R. Hemmati, H. Mehrjerdi, and M. Bornapour, "Hybrid hydrogen-battery storage to smooth solar energy volatility and energy arbitrage considering uncertain electrical-thermal loads," *Renewable Energy,* vol. 154, pp. 1180-1187, 2020.

[12] M. S. Behzadi and M. Niasati, "Comparative performance analysis of a hybrid PV/FC/battery stand-alone system using different power management strategies and sizing approaches," *International Journal of Hydrogen Energy,* vol. 40, no. 1, pp.

[13] G. Correa, F. Volpe, P. Marocco, P. Muñoz, T. Falagüerra, and M. Santarelli, "Evaluation of levelized cost of hydrogen produced by wind electrolysis: Argentine and Italian production scenarios," *Journal of Energy Storage,* vol. 52, p.

[14] Z. Abdin and W. Mérida, "Hybrid energy systems for off-grid power supply and hydrogen production based on renewable energy: A techno-economic

analysis," *Energy Conversion and management,* vol. 196, pp. 1068-1079, 2019.

[15] Y. Zhang, Q. S. Hua, L. Sun, and Q. Liu, "Life Cycle Optimization of Renewable Energy Systems Configuration with Hybrid Battery/Hydrogen Storage: A Comparative Study," *Journal of Energy Storage,* vol. 30, p.

[16] M. Abdulkadir, A. Bukar, and B. Modu, "Mppt-based control algorithm for PV system using iteration-PSO under irregular shadow conditions," *Arid Zone Journal of Engineering-Technology and Environment,* vol. 13, 2017.

[17] S. Singh, M. Singh, and S. C. Kaushik, "Feasibility study of an islanded microgrid in rural area consisting of PV, wind, biomass and battery energy storage system," *Energy Conversion and Management,* vol. 128, pp.

[18] S. Singh, P. Chauhan, and N. Singh, "Capacity optimization of grid connected solar/fuel cell energy system using hybrid ABC-PSO algorithm," *International Journal of Hydrogen Energy,* vol. 45, no. 16, pp. 10070-10088, 2020.

[19] A. Ogunjuyigbe, T. Ayodele, and O. Akinola, "Optimal allocation and sizing of PV/Wind/Split-diesel/Battery hybrid energy system for minimizing life cycle cost, carbon emission and dump energy of remote residential building," *Applied Energy,* vol. 171, pp. 153-171, 2016.

[20] S. Ayub *et al.*, "Analysis of energy management schemes for renewable-energy-based smart homes against the backdrop of COVID-19," *Sustainable Energy Technologies and Assessments,* vol. 52, p. 102136, 2022.

[21] A. Alsharif, C. W. Tan, R. Ayop, M. N. Hussin, and A. L. Bukar, "Sizing Optimization Algorithm for Vehicle-to-Grid System Considering Cost and Reliability Based on Rule-Based Scheme," *ELEKTRIKA-Journal of Electrical Engineering,* vol. 21, no. 3, pp. 6-12, 2022.

[22] J. Zhang and J.-S. Wang, "Improved salp swarm algorithm based on levy flight and sine cosine operator," *IEEE Access,* vol. 8, pp. 99740-99771, 2020.